Electrochimica Acta 78 (2012) 183–187

Contents lists available at SciVerse ScienceDirect

Electrochimica Acta

journal homepage: www.elsevier.com/locate/electacta

The actual current density of gas-evolving electrodes—Notes on the bubble coverage

H. Vogt

Beuth-Hochschule, Berlin, Germany

ARTICLE INFO

Article history:
Received 12 March 2012
Received in revised form 24 May 2012
Accepted 24 May 2012
Available online 15 June 2012

Keywords:
Gas-evolving electrodes
Current density
Bubble coverage
Wettability
Limiting current

ABSTRACT

All investigations of electrochemical reactors with gas-evolving electrodes must take account of the fact that the actual current density controlling cell operation commonly differs substantially from the nominal current density used for practical purposes. Both quantities are interrelated by the fractional bubble coverage. This parameter is shown to be affected by a large number of operational quantities. However, available relationships of the bubble coverage take account only of the nominal current density. A further essential insufficiency is their inconsistency with reality for very large values of the bubble coverage being of relevance for operation conditions leading to anode effects. An improved relationship applicable to the total range is proposed.

1. Introduction

At gas-evolving electrodes, the nominal current density differs from the actual one, since a fraction of the electrode is occupied by adhering gas bubbles and electrochemically inactive. The *nominal* current density is the ratio of electric current and electrode area and can easily be estimated. Therefore, it is a valuable quantity in industrial practice, but it is an artificial quantity inconsistent with reality.

The *actual* current density is always larger than the nominal one. Current flows through an area that is smaller than the geometric electrode surface area. It is the actual current density controlling the overpotential and playing an outstanding role in approaching anode effects in industrial application. Furthermore, the actual current density is the one controlling the ohmic potential drop in the bubble layer adjacent to the electrode. With respect to mass transfer of reactant and product it is a quantity directly affecting the microconvective mass transfer mechanism.

The nominal current density I/A and the actual average current density j are interrelated by

$$j = \frac{I/A}{1-\Theta} \tag{1}$$

where Θ denotes the electrochemically inactive fraction of the electrode surface area. This fraction has been termed bubble coverage when introduced by Ibl and Venczel [1,2]. $(1-\Theta)$ is the fraction of the total electrode surface with an actual (local and temporal) average current density j, whereas the complementary area ΘA is considered currentless.

It can easily be shown [21] that Θ depends on the rate of gas evolution at the electrode and, hence, on the nominal current density. In literature, several equations can be found [3–8] simply interrelating the inactive fraction Θ of the electrode surface with the current density, e.g.

$$\Theta = \left[\frac{I/A}{(I/A)^*}\right]^{0.3} \tag{2}$$

where $(I/A)^*$ denotes a fictitious maximum current density empirically chosen to correlate the experimental data. However, these relationships are not comprehensive enough. A closer look reveals that Θ is controlled by a multitude of impacts. A more general relationship is proposed.

2. Inactive fraction of the electrode surface

The fractional bubble coverage Θ is defined as the number of gas bubbles simultaneously adhering to an electrode surface multiplied with a currentless area appendant to each bubble. Since the bubbles grow during their residence time t_r in contact with the electrode surface, the representative bubble covers an area that is not only

E-mail address: sci@helmut-vogt.de

0013-4686/$ – see front matter © 2012 Elsevier Ltd. All rights reserved.
http://dx.doi.org/10.1016/j.electacta.2012.05.124

List of symbols

A	electrode surface area [m^2]
D_B	diffusion coefficient of dissolved gas [$m^2\ s^{-1}$]
F	Faraday constant, $F = 96{,}487\ A\ s\ mol^{-1}$
f_G	gas evolution efficiency [–]
Fo	Fourier number, Eq. (4)
I	current [A]
$(I/A)^*$	fictitious maximum current density [$A\ m^{-2}$]
$(I/A)_{su}$	summit current density [$A\ m^{-2}$]
j	actual electrode current density [$A\ m^{-2}$]
j_0	exchange current density [$A\ m^{-2}$]
M_B	molar mass of product [$kg\ mol^{-1}$]
n	number of bubbles in contact with electrode
p	pressure [$kg\ m^{-1}\ s^{-2}$]
p_s	vapour pressure of the solvent [$kg\ m^{-1}\ s^{-2}$]
R	radius of growing bubble [m]
R_m	universal gas constant, $R_m = 8.3143\ kg\ m^2\ s^{-2}\ mol^{-1}\ K^{-1}$
R_r	bubble radius at detachment [m]
t	time [s]
t_r	residence time [s]
T	temperature [K]
$\dot{V}_G$	volume rate of gas [$m^3\ s^{-1}$]
V_r	bubble volume at $t = t_r$ [m^3]
α	charge transfer factor [–]
ϑ	contact angle
η	charge transfer overpotential [V]
Θ	fractional bubble coverage of the electrode surface [–]
B	stoichiometric number of product
ν_e	charge number of the electrode reaction
G	gas density [$kg\ m^{-3}$]
Φ_B	current efficiency [–]

an average value of all bubbles on the electrode but also a temporal one.

$$\Theta \equiv \frac{n}{A}\int_0^{t_r} \pi R^2 \frac{dt}{t_r} \tag{3}$$

where R denotes the radius of the average circular area obtained by orthogonal projection onto the electrode surface [4]. n is the number of gas bubbles simultaneously adhering to the electrode area A.

For non-wetting liquids – with a contact angle $\vartheta \geq 90^\circ$ – the inactive area free of current is identical with the contact area. A contact angle $\vartheta \leq 90^\circ$ characterizing wetting liquids means that the radius of the contact area is smaller than the bubble radius. In this case, the definition Eq. (3) is inaccurate, because the current density under the bubble is not zero. However, theoretical estimates by Tobias [9,10] and Müller [11] and their co-workers have shown that the local current density in the immediate surroundings of adhering bubbles is larger than the average and drops to low values as the contact line is approached. The individual current distribution depends on the spacing of adhering bubbles and can be described by the Wagner number [10]. However, the diverging distributions at least partially compensate. Numerical estimates confirm that it is an acceptable approximation to generally equate the equivalent inactive partial area of each bubble with the area obtained by orthogonal projection.

Small bubbles as often encountered at horizontal electrodes facing upwards or vertical electrodes in contact with aqueous solutions have approximately a shape of a truncated sphere. In these cases, the projected radius R equals the spherical bubble radius. Such bubbles approximately grow with a constant Fourier number:

$$\mathrm{Fo} \equiv \frac{D_B t}{R^2} \tag{4}$$

Integration of Eq. (3) with (4) gives

$$\Theta = \frac{\pi}{2}\frac{n}{A}R_r^2 \tag{5}$$

with the radius R_r of the departing bubble. Introducing the volume rate of gas evolution:

$$\dot{V}_G = n\frac{V_r}{t_r}, \tag{6}$$

where V_r denotes the volume of the bubble departing from the electrode, results in

$$\Theta = \frac{\pi}{2}\frac{\dot{V}_G}{A}\frac{t_r}{V_r}R_r^2 \tag{7}$$

For the particular case of a contact angle $\vartheta \to 0$ with

$$V_r = \frac{4}{3}\pi R_r^3, \tag{8}$$

Eq. (7) takes the form

$$\Theta = 0.604\frac{\dot{V}_G}{A}\frac{t_r}{{V_r}^{1/3}} \tag{9}$$

where the flux density of gas evolved into bubbles adhering to the electrode is interrelated with the nominal current density I/A according to Faraday's law under consideration of vapour within the gaseous phase:

$$\frac{\dot{V}_G}{A} = \Phi_B f_G \frac{I/AM_B}{\nu_e/\nu_B F\rho_G}\left(1-\frac{p_s}{p}\right)^{-1} \approx \Phi_B f_G \frac{I/AR_mT}{\nu_e/\nu_B Fp}\left(1-\frac{p_s}{p}\right)^{-1} \tag{10}$$

The gas evolution efficiency f_G denotes the fraction of the total amount of product that is transferred by desorption from the liquid phase into the gaseous phase of adhering bubbles.

3. Quantities acting on the bubble coverage Θ

It is seen from Eq. (9) that the fractional bubble coverage Θ is affected by essentially three quantities:

- the rate of gas evolution at the electrode, $\dot{V}_G/A$,
- the average residence time of bubbles at the electrode surface, t_r,
- the average bubble volume at departure from the electrode surface, V_r.

The quantities within this complex are manifoldly interrelated.

For a given electrode reaction, the rate of gas evolution at the electrode surface, $\dot{V}_G/A$, is controlled by the nominal current density I/A, temperature and pressure, current efficiency Φ_B and gas-evolution efficiency f_G as seen from Eq. (10). The latter parameter is strongly affected by the bubble coverage Θ [12].

The residence time t_r is controlled by the velocity of bubble growth depending on the conditions of mass transfer to adhering gas bubbles, the bubble shape and the concentration of dissolved product in the vicinity of the adhering bubble [13]. The concentration is the result of the nominal current density and the conditions of mass transfer of product from the electrode into the liquid bulk and into the adhering bubbles. Hence, the gas-evolution efficiency plays an important role. It is further on hand, that the residence time depends on the bubble volume V_r reached at departure from the electrode.

This volume depends on shape, size and direction of the operating electrode and may further be largely affected by the conditions of flow of the gas–liquid dispersion near the electrode [14] and

of further impacts such as magnetic forces [15], gravity [16] and supersonic effects [17]. However, aside from these effects, the departure volume is substantially affected by the tendency to coalescence [18] and by the material of the electrode surface and its state [19]. The resulting wettability represented by the contact angle results from the interaction of the interfacial tensions within the 3-phase system electrode surface/electrolyte liquid/gas.

4. Comprehensive relationship of the bubble coverage

Available relationships of the bubble coverage confine to the impact of only one variable, the nominal current density I/A, and ignore all other ones. The result are equations of the type of Eq. (2). Since many more parameters are seen to be of impact, Eq. (2) cannot be satisfying to present the relationship comprehensively.

Establishing a general relationship on the basis of experiments is problematic. For low values of the current density and correspondingly small values of the bubble coverage Θ, visual and optical observation is possible, and numerous experimental data of many authors are available. In this range, the current density I/A was found to result in a monotonical increase in Θ. That is understandable in that increasing current raises the production rate and must result in an increase in the supersaturation of the liquid with dissolved product near the electrode surface, because every increase in the production rate is larger than the corresponding increase in mass transfer. Therefore, increasing current raises the number of active nucleation sites. Although the residence time of adhering bubbles decreases as the current increases (due to increasing growth rate and decreasing departure volume) the bubble coverage Θ increases continuously with the nominal current density.

However, this behaviour is restricted to a lower Θ range. Directly empirical information on the upper Θ range is not available. Experimental difficulties are enormous as the electrode becomes nearly completely covered with adhering bubbles tending to form a continuous gas film. Therefore, for large values of $\Theta \to 1$, experimental data cannot be found in literature. Nonetheless, a statement on the impact of the current density on Θ can be given based on a simple fact: As large values of Θ are attained the gas bubbles are situated close together and the remaining cross sectional area becomes small enough to impede current transport. Any further increase in cell potential (supported by an increase in temperature) results in an increase in Θ, but the resulting current goes down. In the extreme state of a complete gas film, i.e. $\Theta = 1$, the electrode is isolated and the electric current of conventional electrolysis is obstructed. So the current must pass a maximum as the bubble coverage increases from zero to unity.

Hence, it is necessary to extend Eq. (2) for description of the total range, $0 < \Theta < 1$. A semi-empirical relationship based on the experimental data available for the lower Θ range and taking account of the above consideration for the upper range is

$$\frac{I/A - j_0}{(I/A)_{su}} = 3.08\Theta^{1.5}(1-\Theta)^{0.5} \tag{11}$$

where $(I/A)_{su}$ denotes the summit value of the nominal current density as discussed above. The exchange current density j_0 is effective at small values of Θ only.

As seen from Eq. (9) it would have been more adequate to directly insert the rate of gas evolution at the electrode, $\dot{V}_G/A$, into Eq. (11) instead of the current density. Hence, the particular reaction, temperature and pressure would have been taken into account. However, practical handling the equation would have been substantially aggravated. Furthermore, the impact of further parameters represented by the scatter of experimental data is too large to justify such attempts.

For many electrode materials, surface conditions and fields of application the value of $(I/A)_{su}$ appears to be of the order of 10 kA m^{-2}, but may be substantially smaller for extraordinary applications. An appropriate value for certain electrode materials and surface states may be obtained from evaluation of experimental Θ data obtained for low values of the current density.

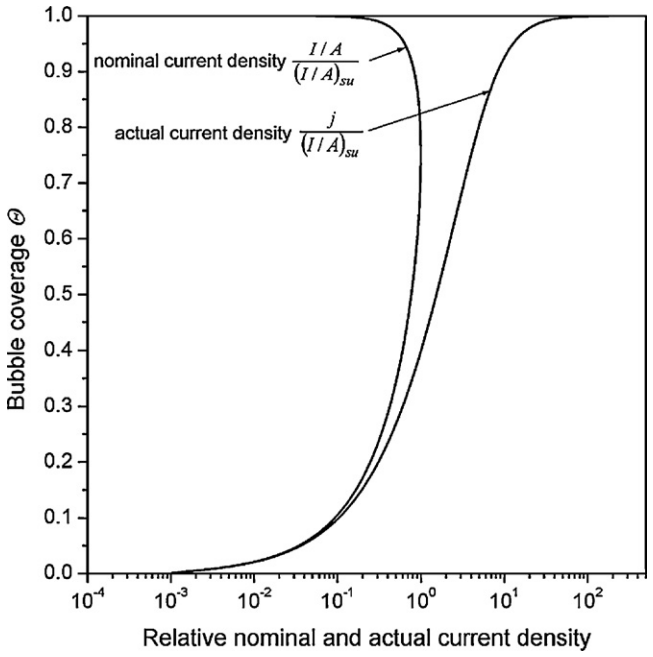

Fig. 1. Relative nominal current density and actual current density vs. bubble coverage.

Eq. (11) is shown in Fig. 1. It is seen that the nominal current density passes a summit value as Θ increases, whereas the actual current density increases monotonically. Although the nominal current density approaches zero, $I/A \to 0$ at $\Theta \to 1$, the actual current density tends to infinity, $j \to \infty$.

For small values of the bubble coverage Eq. (11) reduces to

$$\Theta = \left[\frac{I/A - j_0}{3.08(I/A)_{su}}\right]^{2/3} \tag{12}$$

in formal coincidence with Eq. (2).

Eq. (11) is not quite accurate for extremely large values of bubble coverage, $\Theta \approx 1$, in that in reality a mechanism of completely different type is superimposed: glow discharge is able to proceed through a continuous gas film [20]. So the real electric current at $\Theta = 1$ is somewhat larger than zero. This inaccuracy is irrelevant in application to conventional electrolysis.

Due to the relevance of the bubble coverage Θ on cell operation, numerous experimental investigations have been conducted. Experimental data of several authors for various gases and electrolyte solutions were compiled [21] and are shown in Fig. 2 together with Eq. (11) for three values of the summit current density. The multitude of parameters as discussed in the previous section demonstrates that the scatter of experimental data is not only induced by experimental difficulties.

5. Surface state of electrodes and wettability

The parameter $(I/A)_{su}$ is suitable to take account of most different impacts such as flow velocity of electrolyte liquid, gravity forces and magnetic ones. However, a key role must be attributed to wettability.

Consider two electrodes of same shape, size and direction (e.g. facing upwards) operated at the same conditions such as current density, temperature, pressure, electrolyte concentration, flow

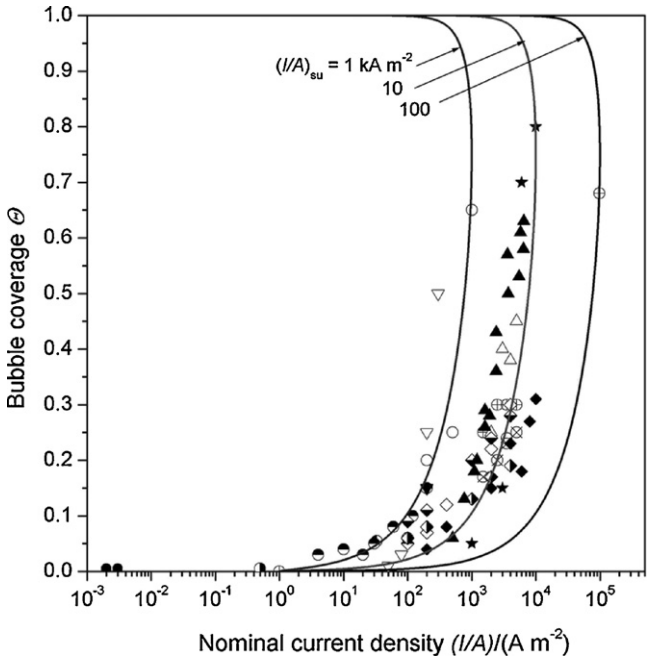

Fig. 2. Nominal current density I/A vs. bubble coverage together with collected experimental data points for aqueous solutions [21], $j_0 = 1\ \mathrm{A\,m^{-2}}$.

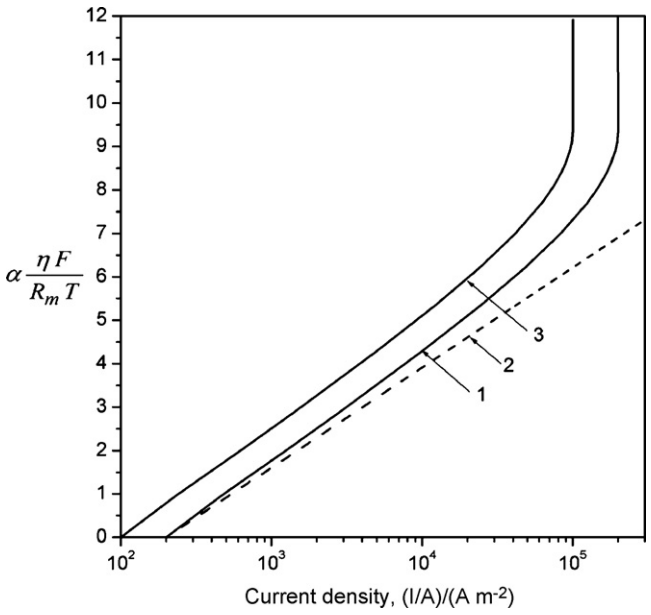

Fig. 3. Calculated anodic overpotential in alumina electrolysis, $j_0 = 200\ \mathrm{A\,m^{-2}}$. 1 – vertical anode surface; 2 – theoretical lines for bubble free electrode; 3 – anode facing downwards.

velocity past the electrode surface, etc. The only difference is the state of the electrode surface in that it acts on the bubble population density. An electrode covered by few bubbles (and low values of the fractional bubble coverage Θ) requires larger current density values to reach the summit current density than an other electrode with poor wettability operated at the same current density with larger values of Θ. Therefore, the parameter $(I/A)_{su}$ in Eq. (11) is predominantly appropriate to represent the surface state of a certain electrode. Any alteration of the physical state acting on the fractional bubble coverage Θ shifts the parameter $(I/A)_{su}$ to larger or smaller values. Large values of $(I/A)_{su}$ are characteristic of strong wettability and smooth surfaces.

Wettability of an electrode surface is subject to various impacts: The interfacial tension at the electrode–liquid interface varies with the potential (electrocapillarity) and acts on the contact angle being an indicator of wetting. Moreover, the surface tension is generally dependent on the concentration. In alumina melts, the contact angle decreases substantially as the concentration of alumina increases inducing serious operation problems [22].

Competing electrochemical reactions may occur as the potential is sufficiently increased due to values of Θ near unity. If such reactions generate a substance that reacts with the electrode material or is deposited at the electrode surface it may act on the wettability [23]. In case of increased contact angle, the inactive fraction Θ of the electrode area increases. Such a case is typical of alumina electrolysis. Discharge of fluorine and reaction with the carbon electrode forms a surface that is definitely associated with a decrease in wetting and a corresponding increase in potential [24,25].

The inactive fraction of the electrode surface may be affected not only by adhering bubbles but also by partial passivation of the electrode surface as a result of electrochemical reactions. In this case, Θ is no longer restricted to the fractional bubble coverage but incorporates an additional passivation effect.

6. Example: production of aluminium

The impact of the bubble coverage of gas-evolving electrodes on the operation of electrochemical reactors may best be demonstrated by an example. In electrolysis of alumina melts in industry as well in laboratory experiments, a fraction of the electrode surface is covered by adhering bubbles. Therefore, the parameter Θ must always be taken into account. Gas bubbles in contact with the electrode do not only increase the ohmic inter-electrode potential drop by forming a bubble layer at the electrode surface. They also act on the anodic charge transfer overpotential which can be written for sufficiently large values of the current density:

$$\alpha\frac{\eta F}{R_{\mathrm{m}}T} = \ln\frac{I}{A(1-\Theta)j_0} - \ln\left(1 - \frac{\nu_{\mathrm{A}}}{\nu_{\mathrm{e}}}\frac{I/A}{Fk_{\mathrm{A}}c_{\mathrm{A}\infty}}\right) \tag{13}$$

Θ appears in the first term representing the very charge transfer overpotential. However, it is also contained in the second mass transfer term although not immediately recognizable, as it is incorporated in the mass transfer coefficient k_{A}.

The predominating mass transfer mechanism at large values of the current density is microconvection [26]. Eq. (13) is shown in Fig. 3 as line 1 for typical operation data applying available mass transfer equations.

For comparison, the Tafel straight line 2 is shown for the fictitious state of $\Theta = 0$. It is seen that the real overpotential at elevate values of the current density is substantially larger than without gas bubbles. That is not surprising since according to Eq. (1) the actual current density j is always larger than the nominal one I/A. It is further seen that estimating the charge transfer factor α from the real slope would lead to a larger value.

In industrial alumina electrolysis, operation conditions are particularly unfavourable in that the anode surface is facing downwards. Release of gas is strongly hampered. Small bubbles easily coalesce to macrobubbles of enormous size under the anode. The fractional bubble coverage attains large values in combined action of the macrobubbles and the much smaller bubbles growing on the active electrode area. In this case the actual current density j on the operating partial electrode area is substantially larger than without macrobubbles at vertical surfaces at the same nominal current density I/A. The corresponding line 3 in Fig. 3 shows larger values of the overpotential than without macrobubbles, line 1. Assessment of the

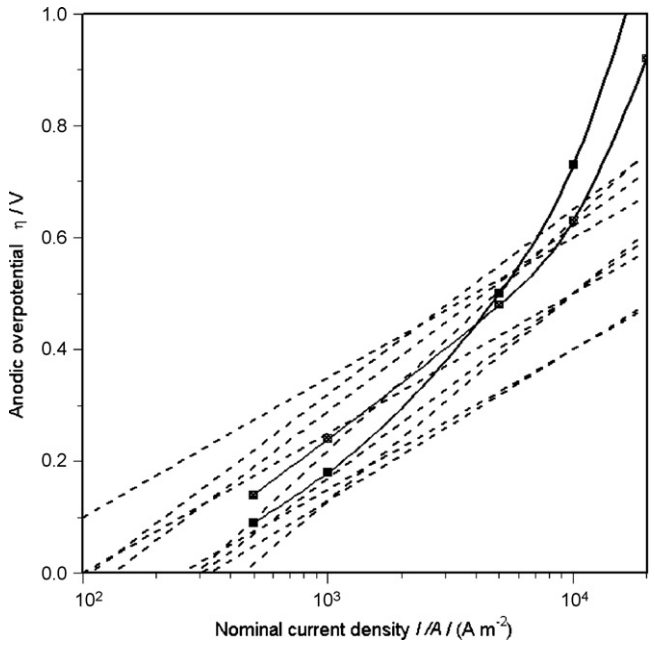

Fig. 4. Anodic overpotential in alumina electrolysis. Experimentally obtained Tafel lines of various authors [27,28] and data points [29].

exchange current density j_0 from experimental data is particularly problematic in this case.

Various experimentally obtained relationships [27,28] representing straight Tafel lines are shown in Fig. 4. Their variety reflects not only the difficulties introduced by variation of the bubble coverage with the current density but also those caused by geometry and orientation of the electrode. By contrast, regression of experimental data points [29] shows curved lines in qualitative agreement with the theoretical lines taking account of the bubble coverage.

7. Conclusions

Available correlations in the form of Eqs. (2) or (12) expressing a monotonical increase in the bubble coverage with the nominal current density are useful only at moderate nominal current densities. Applying these equations to large values of the bubble coverage, i.e. at large values of the actual current density, would lead to results inconsistent with reality.

The relationship Eq. (11) is superior in that it not only applies to small values of the bubble coverage but also takes into account the decay of the nominal current density at very large values. Eq. (11) is recommended for the total range of the current density. It is indispensable for all operation states near the limiting current.

For many applications, empirical values of the important parameter $(I/A)_{su}$ may be used. However, the multitude of impacts prevents predicting reliable values for extraordinary operation conditions. In this case, it must be obtained experimentally from the cell behaviour at moderate values of the current density or estimated in case of substantial variation of wettability during operation.

References

[1] J. Venczel, Über den Stofftransport an gasentwickelnden Elektroden, Thesis, ETH Zurich, 1961.
[2] J. Venczel, Electrochimica Acta 15 (1970) 1909.
[3] P.V. Polyakov, V.M. Mozhaev, V.V. Burnakin, V.A. Kryukovskii, V.E. Nikolaenko, Tsvetnaya Metallurgia 20 (1) (1979) 55;
P.V. Polyakov, V.M. Mozhaev, V.V. Burnakin, V.A. Kryukovskii, V.E. Nikolaenko, Soviet Journal of Non-Ferrous Metals 20 (1) (1979) 46.
[4] H. Vogt, Electrochimica Acta 25 (1980) 527.
[5] C.W.M.P. Sillen, The effect of gas bubble evolution on the energy efficiency in water electrolysis, Dissertation Tech., Hogeschool, Eindhoven, 1983.
[6] H. Vogt, Journal of the Electrochemical Society 137 (1990) 1179.
[7] M.P.M.G. Weijs, L.J.J. Janssen, G.G. Visser, Journal of Applied Electrochemistry 27 (1997) 371.
[8] H. Vogt, Aluminium 74 (2000) 598.
[9] P.J. Sides, C.W. Tobias, Journal of the Electrochemical Society 127 (1980) 288.
[10] J. Dukovic, C.W. Tobias, Journal of the Electrochemical Society 134 (1987) 331.
[11] M. Krenz, L. Müller, A. Pomp, Electrochimica Acta 31 (1986) 723.
[12] H. Vogt, Electrochimica Acta 56 (2011) 1409.
[13] H. Vogt, Electrochimica Acta 29 (1984) 175.
[14] R.J. Balzer, H. Vogt, Journal of the Electrochemical Society 150 (2003) E11.
[15] J.A. Koza, S. Mühlenhoff, P. Zabinski, P.A. Nikrityuk, K. Eckert, A. Gebert, L. Schultz, Electrochimica Acta 56 (2011) 2665.
[16] H. Matsushima, D. Kiuchi, Y. Fukunaka, K. Kuribayashi, Electrochemistry Communications 11 (2009) 1721.
[17] S.-D. Li, C.-C. Wang, C.-Y. Chen, Electrochimica Acta 54 (2009) 3877.
[18] P.J. Sides, C.W. Tobias, Journal of the Electrochemical Society 132 (1985) 583.
[19] H. Vogt, Ö. Aras, R.J. Balzer, International Journal of Heat and Mass Transfer 47 (2004) 787.
[20] P. Gupta, G. Tenhundfeld, E.O. Daigle, D. Ryabkov, Surface and Coatings Technology 201 (2007) 8746.
[21] H. Vogt, R.J. Balzer, Electrochimica Acta 50 (2005) 2073.
[22] H. Vogt, Journal of Applied Electrochemistry 29 (1999) 779.
[23] A. Kailan, Zeitschrift für anorganische Chemie 68 (1910) 141.
[24] V. Schischkin, Zeitschrift fur Elektrochemie 33 (1927) 83.
[25] A. Øygard, T.A. Halvorsen, J. Thonstad, T. Røe, M. Bugge, in: J. Evans (Ed.), Light Metals 1995, The Minerals, Metals and Materials Soc., Warrendale, 1995, p. 279.
[26] H. Vogt, Electrochimica Acta 56 (2011) 2404.
[27] K. Grjotheim, C. Krohn, M. Malinovský, K. Matiašovský, J. Thonstad, Aluminium Electrolysis, Aluminium-Verlag, Düsseldorf, 1977;
K. Grjotheim, C. Krohn, M. Malinovský, K. Matiašovský, J. Thonstad, Aluminium Electrolysis, 2nd edn., Aluminium-Verlag, Düsseldorf, 1982, p. 204.
[28] J. Thonstad, P. Fellner, G.M. Haarberg, J. Hiveš, H. Kvande, Å. Sterten, Aluminium Electrolysis, 3rd edn., Aluminium-Verlag, Düsseldorf, 2001, p. 168.
[29] M.P. Taylor, B.J. Welch, J.T. Keniry, Journal of Electroanalytical Chemistry 168 (1984) 179.